Characterization of the Electrical Resistance of Carbon-Black-Filled Silicone: Application to a Flexible and Stretchable Robot Skin

3 authors:

Marc-Antoine Lacasse
Laval University
10 PUBLICATIONS   **245** CITATIONS

SEE PROFILE

Vincent Duchaine
École de Technologie Supérieure
54 PUBLICATIONS   **1,692** CITATIONS

SEE PROFILE

Clément Gosselin
Laval University
678 PUBLICATIONS   **27,972** CITATIONS

SEE PROFILE

Some of the authors of this publication are also working on these related projects:

Project   Cable-driven robotics, dynamic trajectory planning View project

Project   Master in Robotics View project

Characterization of the Electrical Resistance of Carbon-Black-Filled Silicone: Application to a Flexible and Stretchable Robot Skin

Marc-Antoine Lacasse, Vincent Duchaine and Clément Gosselin

Abstract— **Providing robots with the capability of sensing their surrounding environment is an important feature that would lead to a more intuitive and safe physical human-robot interaction. This paper proposes a new design of homogeneous flexible and stretchable robot skin based on carbon-black-filled (CBF) silicone and conductive fabric that can sense multiple contact locations as well as applied pressure. CBF silicone has been already used in sensing technology but its piezoresistivity is still largely misunderstood. This particular behavior is investigated in this paper through a set of experiments conducted on isolated sensing cells. Using the results of these experiments, a model describing the variation of the resistivity in the CBF silicone as a function of the applied pressure is proposed. Based on this model, a simple way to accurately estimate the applied pressure in real time is demonstrated. Finally, using this improved knowledge of the behaviour of the CBF silicone, the fabrication of a fully functional sensor array is presented. The proposed design has the particularity of circumventing the well-known problem of cross-talk between sensing cells.**

Fig. 1.   Proposed robotic skin with a view of the internal sensor layer.

I. INTRODUCTION

Enabling safe physical human-robot interaction could lead to a new working mode in which human judgment ability and robot power could be efficiently combined. However, due to this specific capability, robots should be designed in a different way in order to ensure the human's physical integrity. One way to make robots safer is by reducing their capability of transferring power. Distributed macro-mini actuation [1], static balancing [2] and torque limiting devices [3] are some examples of proposed solutions in this context. At the sensor level, robots should be able to detect external contacts on their whole body. This capability of sensing contacts would inevitably result in a safer coexistence of humans and robots into the same workspace but would also lead to a more efficient interaction by adding a port of interaction for sensing the human intentions.

An artificial sensitive skin is considered by many as a sensory capability that could lead to more advanced robotics. An increasing amount of work has been done over the last decade on this topic. In [4], the authors present a prototype for collision prevention using infrared sensor pairs(LED + detector) mounted on a polyimide substrate that are able to sense objects at a distance of up to 20 cm. In [5], a more advanced material using organic field-effect transistor featuring pressure sensing capabilities has been proposed. However, this material is still far from commercial

application. In [6], the authors have proposed a realistic solution for industrial applications based on a pressure-activated conductive rubber sheet to sense multi contact locations. The reported experiments have shown that using a skin with such a simple feature can greatly improve safety in human-robot interaction by detecting collisions and reacting to them. However, despite this success, determining only contact location does not address the problem of intuitive collaboration, since such primary information is clearly not sufficient for making a distinction between wanted or unwanted contact. Adding pressure sensing capabilities will help filling this gap.

An inherent property of Carbon-black-filled silicone (CBF silicone) makes this material a good candidate for playing this role, especially if high precision is not required. Indeed, the electrical resistivity of CBF silicone changes with the applied pressure. Moreover, its viscoelastic behaviour add compliance that greatly helps dissipating contact energy. Unfortunately, nonlinearity, creep and long relaxation time make it difficult to estimate the applied pressure. In [7], the authors suggested that the relation between pressure and internal resistance is similar to the stress/strain relation of a viscoelastic material. In a similar way, [8] used the Burgers viscoelastic model to fit the resistive behaviour during compression. Although these models help to predict the time-resistivity behaviour of loaded silicone, work has to be done in order to estimate the applied load from the time-resistivity output. CBF silicone has already been used in the design of pressure sensitive sensors as in [9] where row and column electrodes have been stitched across a one piece sensor layer. However, while the simplicity of the
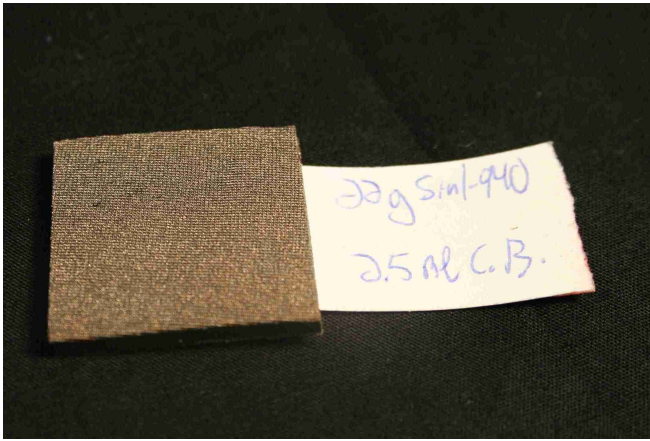
Fig. 2. Sample used in the investigation of the optimal sensitivity and for the characterization of the resistivity behaviour.

approach was promising for realistic full scale applications, the resulting sensor was subject to the well-known cross-talk effect, which produces an unwanted variation at a given sensing point for a pressure applied at another point.

This paper presents a new simple and cost-effective design of flexible and stretchable robot skin. The sensor array based on carbon-black filled (CBF) silicone and conductive fabric, is built in a way that even if the resulting material is homogeneous, each tactile cell is isolated from the others to prevent cross-talk. First, a study on the sensitivity of a single sensing cell is conducted in order to find the optimal mass ratio of carbon black versus silicone. Using the resulting optimal sample, the change of the resistivity of the CBF silicone in reaction to an applied pressure is investigated to gain a better understanding of the overall sensor behaviour. Based on these results, a model is defined and further used to estimate the applied pressure on a sensing cell in real-time. Finally, the fabrication of a fully functional sensor array that can detect multi-contact locations as well as pressure is presented. Fig. (1) shows a picture of the resulting robot skin.

II. CARBONE-BLACK-FILLED SILICONE PREPARATION

The electrical properties of CBF silicone vary depending on the nature and the proportion of the two materials. This section investigates the problem of finding the optimum concentration of carbon in a given platinum silicone that will lead to the maximum sensitivity.

A. Method

For the sensitivity test, Smooth-Sil 940, a two-part platinum cured silicone was mechanically mixed for two minutes, without any solvent, with carbon black powder(carbon black, acetylene, 50% compressed, 99.9+% (metal basis)) from Alfa Aesar. The mixture cured at room temperature during 4 hours in a 0.125 thickness mold and was then cut into one square inch samples. Stretchable conductive fabric ($0.1\Omega/cm$) made by *Les EMF* was embedded into each cell to serve as an electrode in the material. Fig. (2) show one of the samples used for this experiment.

B. Optimization of sensitivity

We define the sensitivity of CBF silicone as the following ratio : $(R_{max} - R_0)/R_0$ where R_0 is the initial resistivity and R_{max} is the resistivity at which the output signal saturates. A good sensitivity makes the data processing easier by reducing the relative noise level and the error due to the discretization of the input signal. Using the fabrication method previously described, eight samples were prepared with various carbon black mass fractions and their sensitivity was measured. Fig. (3) shows the normalized resitance variation ($(R_{max} - R_0)/R_0$) for these samples. It appears that the sensitivity of
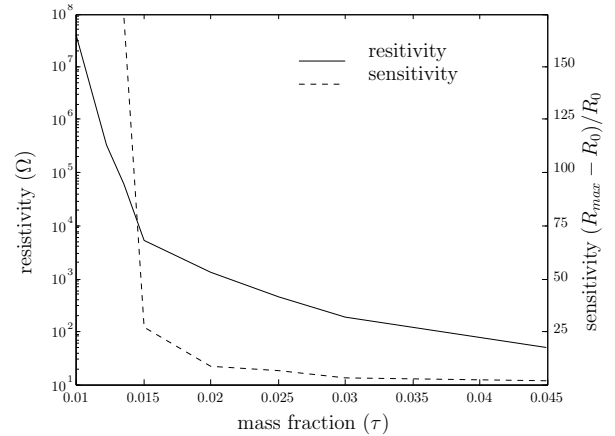

Fig. 3. Resistivity and sensitivity of Smooth-Sil 940 silicone composite as a function of CB mass fraction.

the silicone increases when the CB mass fraction decreases. The experiment stopped at 1.5% but there is most likely a mass fraction in the range between 0% and 1.5% that would lead to a better sensitivity. However, with the mass fraction approaching zero, the maximal resistivity tends to ∞, thereby driving not enough current for the acquisition system. Therefore, as a compromise between sensitivity and hardware limitation, a 1.5% CB mass fraction is chosen for the design of the sensing device.

III. PRESSURE SENSITIVE RESPONSE MODEL

Several papers [10], [11], [12] have been written about the electrical properties of pressure sensitive rubber composite using silicone and carbon black. Some of them [10] observed a decrease of the electrical resistivity when a pressure is applied. One generally accepted idea to explain this phenomenon is the compressive matrix model. This concept considers the volume of CB to be constant, by contrats with the volume of silicone that decreases with pressure. Therefore, the volume fraction of CB increases under the load, which induces a drop of electrical resistivity. In other words, since the overall sensor volume decreases, more contact is made between conductive particles, leading to a decrease of the internal resistance.

Other researchers [13], [14] have observed the opposite effect, i.e, an increase of the resistance under an applied load. One proposed explanation for this variation is given by an alternative mode in which the silicone is considered as

Effectives conductives paths

(a) Compressible model in which volume fraction of CB increases leading to new effective conductive path.

(b) Incompressible model where small displacements lead to reversible destruction of effective conductive paths.
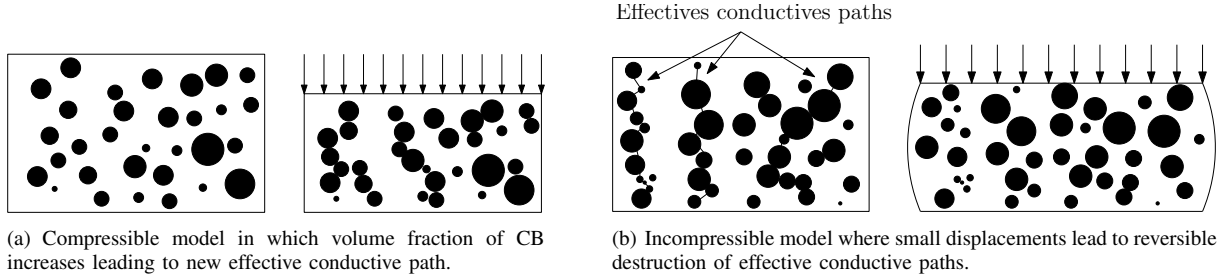
Fig. 4. Comparison of two important models to explain the resistance variation of CBF silicone under pressure. Both phenomena probably occur inside silicone and their predominance depends on the filler material and the nature of the polymer matrix.

incompressible (but deformable) material. In this concept, the effective conductive paths are broken by the matrix deformation, leading to an increase of resistivity along with pressure. Fig. (4a.) and Fig. (4b.) respectively illustrate these two models.

From our experiments, we have observed both types of resistance variation with the same CBF silicone mixture, depending on the nature of electrode contact. Fig. 5 shows the change of resistivity of two samples both built with 1.5% CB. Both samples use the same conductive fabric electrode. For the lower curve, the electrode was cast inside the silicone compared while for the other one the electrodes were not bound to the CBF silicone.
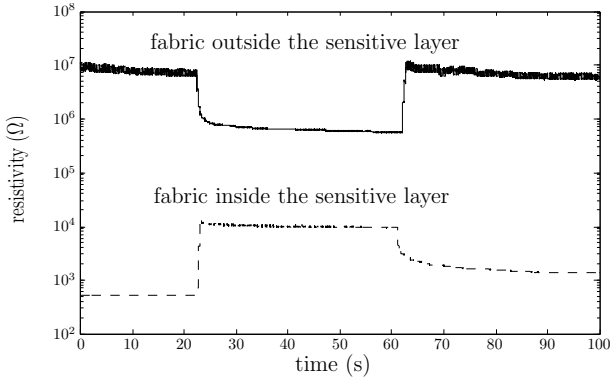

Fig. 5. Change in resistivity of CBF silicone depending on the nature of electrode contact.

This experiment suggests that the case for which the resistance decreases when going form an unloaded to a loaded state is linked with the contact resistance rather than with the real internal CBF resistance. If the electrodes are outside, an increase in the applied pressure on the material will increase the contact area and the resistance will decrease. This could explain why, in Fig. 5 the curve for the specimen with outside electrodes does not react like a viscoelastic material. Since the contact resistance is a lot larger than the material resistivity, the effect of resistance variation of the material itself does not appear on the curve with outside conductive fabric electrodes. When the electrodes are inserted in the silicone mixture, contact resistance becomes negligible and therefore the variation of the resistance reflects the variation of the resistance of the CBF silicone itself. The resistance

variation of the CBF silicone presented in this article better fits the incompressive model in which matrix deformation breaks effective conductive paths that are recovered as the material returns to its original configuration.

IV. MODELLING OF THE RESISTIVITY BEHAVIOUR

As seen in the above section, the variation of the resistivity of the CBF silicone used in the design of the proposed robotic skin follows a curve similar to the strain (ϵ) in a viscoelastic material. While for elastic material, the stress (σ) is directly linked to the strain (ϵ) via Young's modulus (E), for a viscoelastic material this relation can be much more complex [15]. One impact of this is a non-instantaneous recovery when going from a loaded state to an unloaded one. For example, with the prototype presented in this paper, looking at the resistivity (R) of the material, it can take up to 25 seconds to reach 95% of recovery after unloading the skin. A robot that would be controlled based on this signal would inevitably produce unwanted motion. Therefore, it is essential to define an appropriate model of the resistivity variation of CBF silicone that could be used to predict the real pressure applied on the skin. Knowing that :

$$R \propto \epsilon, \tag{1}$$

the modelling exercise can be summarized as finding a function such as :

$$R = f(\sigma). \tag{2}$$

Some authors [8], [16],[7] have investigated this relation. However, the proposed model was function of time, which can be difficult to deal with in a real-time implementation aiming at making input prediction. Moreover, these papers only investigated the response in the recovery phase. As it can be seen in Fig. (6), the initial response to a pressure unit step greatly differs from the one in the recovering phase, leading to a nonlinear overall resistivity behaviour of the CBF material. In this work, these two phases will be analyzed using two distinct models.

A. Rising phase

A typical rising response to a unit step is shown in fig. (6). As it can be seen, this phase is mainly characterized by a quasi instantaneous response to an applied pressure then followed by a small and slow restitution that will tend toward an
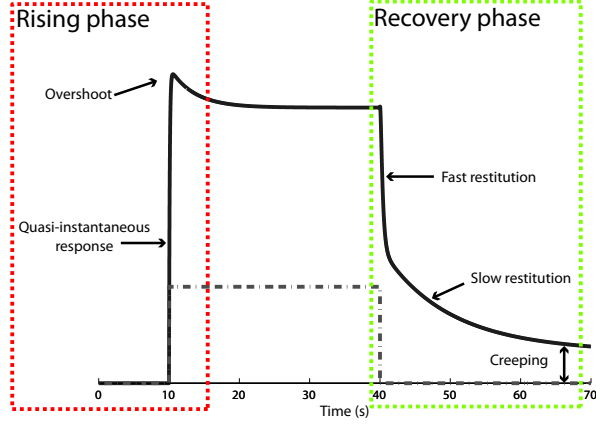
Fig. 6. Typical resistance variation curve for a pressure step applied.

Fig. 7. Augmented Burger model.

equilibrium value. As suggested in [17], this abrupt change in the resistivity and the following overshoot of the equilibrium point can be caused by the instantaneous destruction of the conductive chains followed by a reformation process.

Several tests performed with the sensitive cells suggested that this phase can be accurately approximated by a combination of a simple gain together with a first order transfer function between the resistivity (R) and the first time derivative of the stress ($\dot{\sigma}$). In the Lapace domain, this gives :

$$G_{up}(s) = \frac{1}{E_{u1}} + \frac{s}{\eta_{u2}s + E_{u2}} = \frac{(E_{u1} + \eta_{u2})\,s + E_{u2}}{E_{u1}\eta_{u2}s + E_{u1}E_{u2}}. \quad (3)$$

B. Recovery phase

[15] As it can be seen from fig. (6), the recovery process has very slow dynamics as opposed to the rising phase and varies similarly to the strain in a viscoelastic material during relaxation. The latter aspect has been studied by many and it is known to be a combination of different effects, i.e, elastic behaviour (high dynamics component), viscoelastic response(slow dynamics component) and viscous response (creep). The Burgers model [18], which is a combination of a Maxwell model (spring and dashpot in series) and a Kelvin-Voigt model (spring and dashpot in parallel), can accurately model this behaviour by taking into account these three different effects.

As mentioned above, the variation of the resistivity of the CBF silicone during the recovery phase follows very closely the strain in the material. However, it differs on one small aspect. While the creep typically prevents a return of the material to its initial displacement, the resistivity in our tests seem to be a recoverable process that always returns to its original value. However, the time needed to return to the initial resistance can be relatively long (up to 5 minutes) and thus, over a short period of time, it is easy to confuse this slow recovery with a residual strain. To include this particularity, an augmented Burgers model, was used. In what we have called the five elements model, a spring has been added to the serial dashpot that usually accounts for the creep
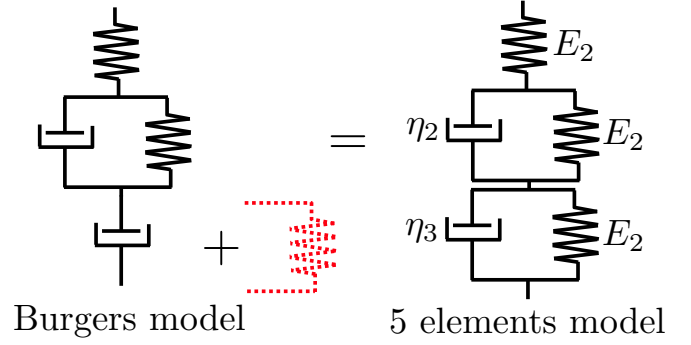
in the material. This spring has the effect of always taking the resistance back to its original value. Fig. (7) illustrates our model and how it differs from the Burger model.

The representation in the Laplace domain of this model that links the resistivity of one skin cell r_i to the applied stress σ_i on this cell is written as :

$$G(s) = \frac{R(s)}{\sigma(s)} = \frac{as^2 + bs + c}{\eta_2\eta_3s^2 + (\eta_2 E_3 + \eta_3 E_2)\,s + E_2E_3}, \quad (4)$$

with

$$a = \frac{\eta_2\eta_3}{E_1} \quad (5)$$

$$b = \frac{E_2\eta_3 + E_3\eta_2}{E_1} + \eta_2 + \eta_3 \quad (6)$$

$$c = \frac{E_2E_3}{E_1} + E_2 + E_3. \quad (7)$$

1) Determination of the Model Coefficients: The first step before using the above equations is finding the values of the coefficients E_i and η_i appearing in eq. (3) and eq. (4). Notice that these coefficients have no physical meaning since their values depend on a normalized resistance. Finding the coefficients for the rising phase is rather straightforward since the model is close to be a simple gain. However, the parameters of the recovery model can be more tricky to find. One way to do it is by separating eq. (4) into a sum of functions representing its three original serial components, namely an elastic model and two visco-elastic models :

$$G(s) = \frac{R(s)}{\sigma(s)} = \frac{1}{E_1} + \frac{1}{\eta_2s + E_2} + \frac{1}{\eta_3s + E_3}. \quad (8)$$

Thereafter, E_1, E_2 and E_3 can be found as the inverse of the respective gain for each associated phase of the recovery curve. Then, by observing the decreasing dynamics of each phase, the associated time constant (T_i) can be inferred to find η_2 and η_3 such that :

$$\eta_i = T_i E_i. \quad (9)$$

Fig. 8 shows the effect of each serial component to a released pressure and the total response as the combination of them.
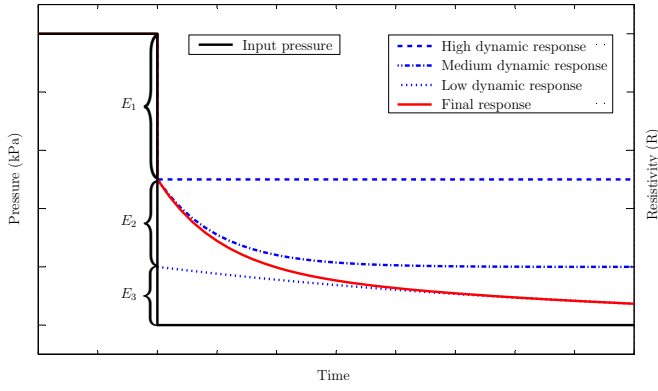
Fig. 8. Typical response to a released pressure and curves of serial components for the corresponding model.

V. ESTIMATION OF THE INPUT PRESSURE

The models presented above describe the change in resistivity in the CBF material. However, the real need for these models is the determination the currently applied pressure on a given sensing cell. This implies inverting the above equations. The Laplace transfer functions given by eq. (3) and eq. (4) have the particularity of being of the same order in both the numerator an the denominator. Therefore, once the coefficients E_i and η_i of eq. (3) and eq. (4) are known, these functions only have to be inverted and used as a filter where the value of the resistivity is the input and the applied pressure is the output. One remaining challenge is deciding
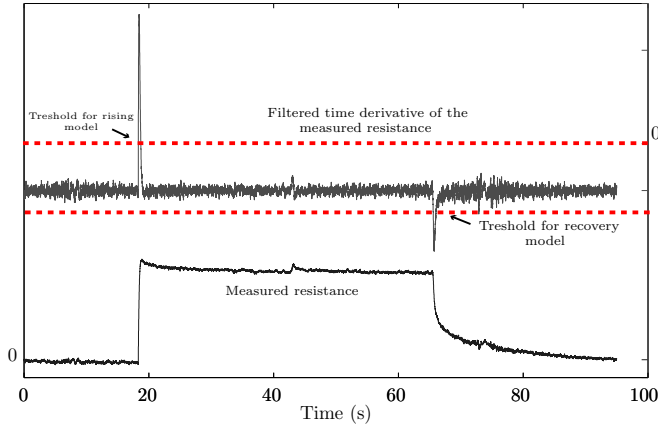

Fig. 9. Time derivative of the measured resistance and how it can be used for switching between the two prediction models.

which of the two models to use. As seen above, the resistivity behaviour of the used material cannot be modeled with a simple linear equation. Therefore, one model was defined for the rising response while another one was defined for the recovery phase. Hence, the prediction of the applied pressure obtained when inverting each model will only be valid in their respective circumstances. Thus, for adequately estimating the applied pressure, the prediction should be made by alternating judiciously between each model according to their respective domain of validity. One way to know when the rising model or the recovery model should be used is by
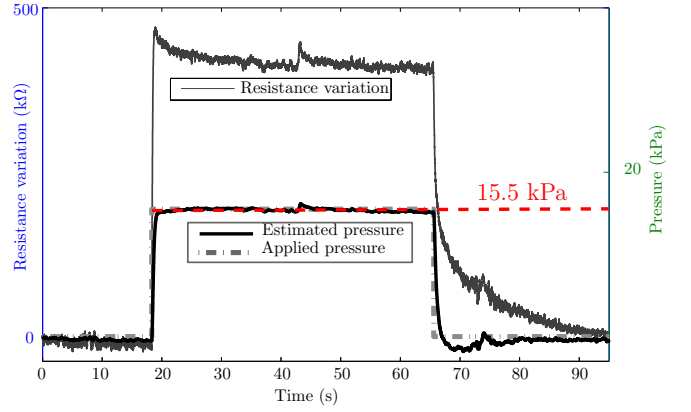

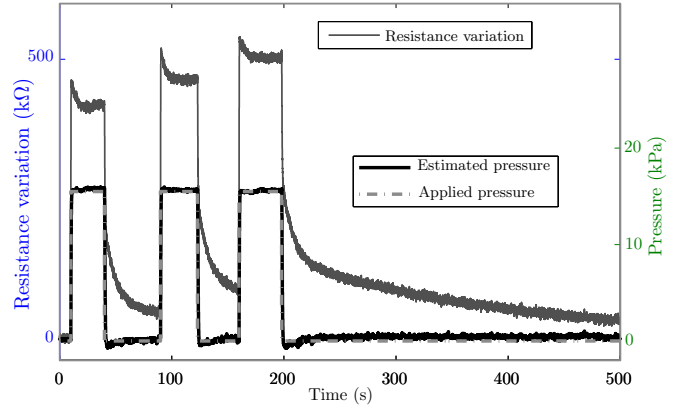Fig. 10. Resistance variation to an applied step of pressure and the resulting stress estimation.

Fig. 11. Three successive pressure steps applied and the resulting creep.

monitoring the time derivative of the resistance. If the time derivative is above a given positive threshold, the prediction should be based on the rising phase equation while if the time derivative is below another negative threshold, the filter should be set using the recovery phase model. Fig. (9), taken from a real experiment, shows how the derivative of the input signal (ρ_i) can be used for deciding which of the two models should be used.

A. Validation

Fig. (10) shows the effectiveness of the proposed method at adequately predicting the actual stress on the material. For this test, a pressure of 15.5 kPa was applied and released on one sensing cell. The response to this step was used to define the visco-elastic coefficients (E_i and η_i) for each model. Thereafter, the equations were used (the derivative of the resistance was used to select the proper model) to infer the actual stress in the material. As seen on the curves, this model can adequately compensate for the slow dynamics during recovery of the sensing material. This test was repeated with three successive pressure steps, to demonstrate the effect of the creep. Fig. (11) shows the obtained resistance curve and the resulting estimation of the stress. Even with creep, if coefficients E_3 and η_3 are properly defined, the model can still reasonably predict the stress in the material.

VI. Skin fabrication process

The previous sections investigated the properties and the behaviour of the CBF silicone using a single sensing cell. This section presents how a complete sensor array can be produced using this material. A simple method based on Shape Deposition Manufacturing [19] was developed that aims at minimizing the number of required successive casts in order to keep the production time as short as possible.

A. Conductive fabric circuit

As mentioned above, in order to obtain a stretchable and flexible robot skin, the conductive array in the skin is made of a conductive fabric. The fabric is preliminarily cut into several discrete cells in order to form a conductive array and then the resulting circuit is mounted on a polyimide sheet with an adhesive back. The polyimide film and its adhesive do not bond or react with silicone and thus, this thin film is used to mask part of the circuit that should not stick to the silicone. This masking process is performed on both sides of the sensor.

B. Casting of the sensitive part

The next step is to cast the CBF silicone between the two conductive fabric circuits at the optimal concentration defined above. For this step, the rows and columns of the sensor array are carefully aligned perpendicularly, since it will not be possible to further move these part. Fig. 12 a) illustrates this step.

C. Slicing of the CBF silicone

Once the silicone is cured, the material is sliced to remove the extra CBF material between each row and column in order to obtain discrete sensing cells. This step is facilitated by the polyimide mask that was previously placed on the conductive fabric where silicone has to be removed. The sensor could be functional without this step, but isolating each sensing cell from the others avoids the cross-talk between the cells. Fig. (12 b.) shows the result of this step.

D. Final packaging of the sensor layer

In order to obtain a homogeneous sensor layer, the resulting assembly is then embedded into a silicone layer also made of non-conductive Smooth-Sil 940. Since the conductive fabric has been cast directly into the CBF silicone, there is no chance for the non-conductive silicone to form an insulating film between the sensitive part and the electrodes. Fig. (12 c.) shows the final result of the sensor layer.

E. Complete skin

To make the skin more robust, and to add compliance that will help to dissipate collision energy, a final protective layer minus thickness (1/16 inch) than the sensor part is cast. Fig. (1) gives an overview of the resulting complete skin.

VII. Acquisition system

A robot skin cannot be used without a proper data acquisition system. For a single sensitive cell, a voltage divider and an analog to digital system could be used to obtain a signal proportional to the resistivity of the sensor. For a complete sensor structure, crosstalk currents make it difficult to use such a circuit. From Fig. 13 we see that, when trying to estimate the resistance R_{11}, current could pass through many other paths than R_{11}. For example, current could pass through R_{21}, R_{24} and R_{14} to return to the ground. Hence, the resistivity estimated would be the one of the equivalent grid resistor.
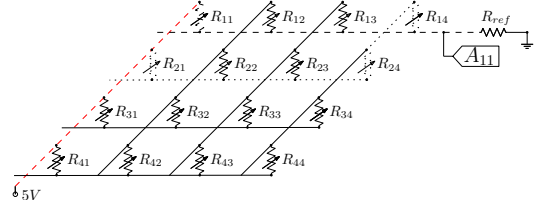

Fig. 13. Equivalent grid resistance of robot skin and possible crosstalk currents.

To avoid crosstalk current, the electrical potential of all rows and columns, which are not the one to be selected should be equal, thereby preventing crosstalk currents. Following the idea, an elegant solution was found in [20] in order to obtain a signal depending only on R_{ij}. In the latter reference, the negative feedback of an operational amplifier is used to reduce the voltage of the driven column to the ground. Fig. 14 shows the circuit, which is a simple inverting amplifier. As no current enters the inverting input, $i_{R_{ij}} = i_{R_{ref}}$ and we find easily the relation between the input and the output, namely :

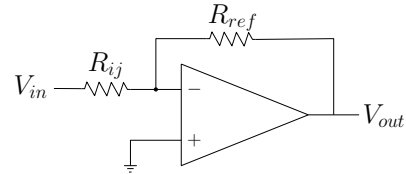$$V_{out} = -V_{in} \left(\frac{R_{ref}}{R_{ij}} \right) \qquad (10)$$

Fig. 14. Circuit of the inverting amplifier used as a voltage divider to estimate R_{ij}.

By using such a circuit on each column and grounding every row that is not driven, we can estimate the value of R_{ij} without any crosstalk effect. Fig. 15 shows the concept for the complete scanning circuit.

VIII. Conclusion

The capability of sensing contact on the whole body of a robot is clearly a key feature for enabling safe and more advanced physical human-robot interaction. In this paper, a new design of a flexible and stretchable robot skin that

(a) Conductive fabric circuit (b) Removal of undesirable conductive silicone (c) Complete skin
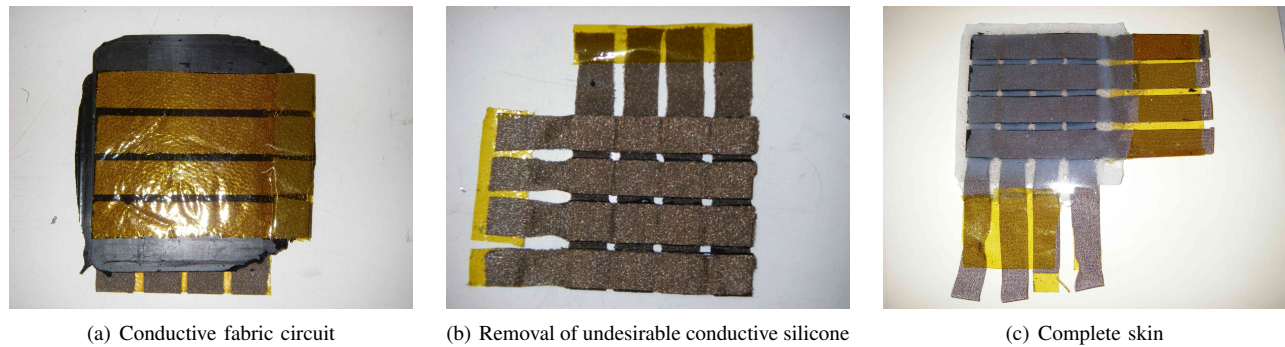
Fig. 12. Fabrication process of a stretchable and flexible robot skin.
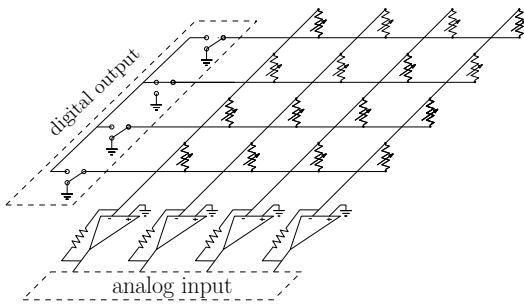

Fig. 15. Scanning circuit for a four by four robot skin prototype.

can detect multi-contact locations as well as pressure level was presented, with the aim of providing this capability to robots. The fabrication process of this new sensor based on carbon black filled silicone was first reviewed and then the behaviour of the sensing layer was analyzed. Indeed, even if CBF silicone has been already used in some sensor technology, its piezoresistive behaviour is still largely misunderstood. We have shown that using this material with bond or unbond electrodes can lead to completely opposite resistivity behaviour due to the contact resistance between the electrodes and the CBF silicone. Finally, based on our design where conductive layers are perfectly merged with the CBF silicone, a model was proposed to characterize the variation of the internal resistivity for an applied pressure. Using the inverse of this model in conjunction with the current resistance value, it was shown that it is possible to accurately estimate the applied pressure. Finally, a prototype of a flexible and strechable robot skin based on the sensor array was described.

REFERENCES

[1] M. Zinn, O. Khatib, and B. Roth, "A new actuation approach for human friendly robot design," in *2004 IEEE International Conference on Robotics and Automation, 2004. Proceedings. ICRA'04*, vol. 1.

[2] N. Lauzier, C. Gosselin, T. Laliberté, and P. Tremblay, "Adaptive gravity compensation of decoupled parallel and serial manipulators using a passive hydraulic transmission," *Proc. IMechE Vol. 223 Part C : J. Mechanical Engineering Science*, vol. 1, 2009.

[3] J.-J. Park, B.-S. Kim, J.-B. Song, and H.-S. Kim, "Safe link mechanism based on passive compliance for safe human-robot collision," pp. 1152–1157, May 2007.

[4] V. J. Lumelsky, M. S. Shur, and S. Wagner, "Sensitive skin," *Sensors Journal, IEEE*, vol. 1, no. 1, pp. 41–51, 2001.

[5] T. Someya, T. Sekitani, S. Iba, Y. Kato, H. Kawaguchi, and T. Sakurai, "A large-area, flexible pressure sensor matrix with organic field-effect transistors for artificial skin applications," *Proceedings of the National Academy of Sciences of the United States of America*, vol. 101, pp. 9966–9970, July 2004.

[6] V. Duchaine, N. Lauzier, M. Baril, M. Lacasse, and C. Gosselin, "A flexible robot skin for safe physical human robot interaction," in *Robotics and Automation, 2009. ICRA '09. IEEE International Conference on*, pp. 3676–3681, 2009.

[7] J. Kost, A. Foux, and M. Narkis, "Quantitative model relating electrical resistance, strain, and time for carbon black loaded silicone rubber," *Polymer Engineering & Science*, vol. 34, no. 21, pp. 1628–1634, 1994.

[8] T. Ding, L. Wang, and P. Wang, "Changes in electrical resistance of carbon-black-filled silicone rubber composite during compression," *Journal of Polymer Science Part B : Polymer Physics*, vol. 45, no. 19, pp. 2700–2706, 2007.

[9] M. Shimojo, A. Namiki, M. Ishikawa, R. Makino, and K. Mabuchi, "A tactile sensor sheet using pressure conductive rubber with electrical-wires stitched method," *Sensors Journal, IEEE*, vol. 4, no. 5, pp. 589–596, 2004.

[10] M. Hussain, Y. Choa, and K. Niihara, "Fabrication process and electrical behavior of novel pressure-sensitive composites," *Composites Part A : Applied Science and Manufacturing*, vol. 32, pp. 1689–1696, December 2001.

[11] C. A. González-Correa, G. Screaton, D. R. Hose, B. H. Brown, N. J. Avis, and F. Kleinermann, "Resistivity changes in conductive silicone sheets under stretching.," *Physiological measurement*, vol. 23, pp. 183–188, February 2002.

[12] D. Beruto, M. Capurro, and G. Marro, "Piezoresistance behavior of silicone -graphite composites in the proximity of the electric percolation threshold," *Sensors and Actuators A : Physical*, vol. 117, pp. 301–308, January 2005.

[13] L. Wang, T. Ding, and P. Wang, "Effects of instantaneous compression pressure on electrical resistance of carbon black filled silicone rubber composite during compressive stress relaxation," *Composites Science and Technology*, vol. 68, pp. 3448–3450, December 2008.

[14] W. Min, H. Ying, G. Yunjian, F. Xiulan, and H. Panfeng, "A study of resistance relaxation phenomenon based on carbon black/silicone rubber system flexible tactile sensor," in *Information Acquisition, 2007. ICIA '07. International Conference on*, pp. 366–371, 2007.

[15] K. Menard, *Dynamic mechanical analysis : a practical introduction*. CRC, 2008.

[16] L. Wang, T. Ding, and P. Wang, "Research on stress and electrical resistance of skin-sensing silicone rubber/carbon black nanocomposite during decompressive stress relaxation," *Smart Materials and Structures*, vol. 18, no. 6, p. 065002, 2009.

[17] J. Kost, M. Narkis, and A. Foux, "Resistivity behavior of carbon-black-filled silicone rubber in cyclic loading experiments," *Journal of Applied Polymer Science*, vol. 29, no. 12, 1984.

[18] N. Heymans, "Hierarchical models for viscoelasticity : dynamic behaviour in the linear range," *Rheologica Acta*, vol. 35, no. 5, pp. 508–519, 1996.

[19] M. Hatanaka and M. Cutkosky, "Process planning for embedding flexible materials in multi-material prototypes," *DETC ASME, Chicago, Illinois, USA, September*, 2003.

[20] M. Shimojo, A. Namiki, M. Ishikawa, R. Makino, and K. Mabuchi, "A tactile sensor sheet using pressure conductive rubber with electrical-wires stitched method," *Sensors Journal, IEEE*, vol. 4, no. 5, pp. 589–596, 2004.